Plasmid 104 (2019) 102419

Contents lists available at ScienceDirect

Plasmid

journal homepage: www.elsevier.com/locate/yplas

Original Research Article

Assembly of large mobilizable genetic cargo by double recombinase operated insertion of DNA (DROID)

Kevin Neil[a], Nancy Allard[a], David Jordan[a], Sébastien Rodrigue[a,b,*]

[a] Department of Biology, University of Sherbrooke, Sherbrooke, QC J1K 2R1, Canada
[b] Centre de recherche du CHUS, Sherbrooke, QC J1H 5N4, Canada

ARTICLE INFO

Keywords:
DNA assembly
Plasmid
Conjugation
CRISPR-Cas9
Recombinase

ABSTRACT

There is an important need to develop new therapeutic tools to modulate the gene content of microbiomes. A potential strategy for microbiome engineering relies on the delivery of genetic payloads by conjugative plasmids. Yet, the introduction of large DNA molecules in conjugative plasmids can be challenging. Here, we describe the Double Recombinase Operated Insertion of DNA (DROID), an efficient method to assemble large DNA molecules without introducing antibiotic resistance genes or other unwanted sequences in the final construct. We exemplify this method by demonstrating that the Bxb1 integrase and FLP recombinase can be used successively to stably insert a relatively large DNA cargo consisting of a CRISPR-Cas9 system in a conjugative plasmid. We further show that the resulting CRISPR-Cas9 mobilization system was able to cure a multi-copy antibiotic resistance plasmid in a target bacterium. In addition to its utility for DNA payload integration in conjugative plasmids, the DROID method could readily be adapted to a multitude of other applications that require the manipulation of large DNA molecules.

1. Introduction

Many estimates suggest that the human body hosts a greater number of micro-organisms than human cells (Sender et al., 2016). These micro-organisms form the microbiota and play key roles in several processes such as nutrient absorption (Ley et al., 2005), host metabolism (Bäckhed et al., 2007), defense against pathogens (Cash et al., 2006), drug processing (Guthrie et al., 2017), *etc.* However, repeated infections and antibiotic treatments can lead to the accumulation of antibiotic resistance and virulence associated genes (Penders et al., 2013). Furthermore, the gut microbiota is a suspected hot-spot for horizontal gene transfer, hence promoting the dissemination of potentially harmful genes between bacteria (Van Schaik, 2015). New tools to modulate the composition of the microbiome could offer a powerful avenue to prevent or treat antibiotic resistant infections and dysbiosis.

One promising way to engineer the microbiome is through the delivery of DNA payloads to the microbiota residents using either bacteriophages or conjugative plasmids. For example, phage-based delivery was used to transfer CRISPR-Cas9 systems and eliminate antibiotic resistant pathogens (Bikard et al., 2014; Citorik et al., 2014) or to resensitize them to antibiotics (Yosef et al., 2015). Both bacteriophages and conjugative plasmids have advantages and inconvenients for DNA delivery. While phage-based systems can reach high DNA transfer efficiencies, they often present narrow host range (Villarroel et al., 2016), limited DNA payload size (Nurmemmedov et al., 2012) and susceptibility to conditions found in the gut environment (pH, bile salts, proteases) (Nobrega et al., 2016). In contrast, conjugative plasmids are often large DNA molecules that can accommodate DNA payloads of considerable sizes and transfer to a large variety of hosts. Conjugative plasmids therefore have the potential to mobilize larger constructs, such as biosynthetic pathways and complex DNA circuits to supplement deficient functions in an imbalanced microbiota. Yet, efficiently loading large DNA payloads (*e.g.* CRISPR-Cas9) into phages and conjugative plasmids remains challenging.

Several methods have been described to mediate the association of two or more DNA molecules *in vitro*. For example, Gibson assembly (Gibson et al., 2009), digestion-ligation (Cohen et al., 1973), Golden Gate (Engler et al., 2008), USER-cloning (Geu-flores et al., 2007) are commonly used but the assembly of large DNA molecules often remains challenging. Indeed, the efficiency of these techniques quickly drops

Abbreviations: bp, Base pair; Cm, Chloramphenicol.; DROID, Double Recombinase Operated Insertion of DNA.; EcN, *Escherichia coli* Nissle 1917.; IncI2, Incompatibility Group I2.; Km, Kanamycin.; LB, Luria Broth Miller.; LBA, Luria Broth Miller Agar.; OD_{600nm}, Optical Density at 600 nm.; PAM, Protospacer Adjacent Motif.; pT, Target plasmid.; pNT, Non-Target plasmid.

* Corresponding author at: Département de biologie, Université de Sherbrooke, 2500 Boulevard de l'Université, Sherbrooke, QC J1K 2R1, Canada.
E-mail address: Sebastien.Rodrigue@USherbrooke.ca (S. Rodrigue).

https://doi.org/10.1016/j.plasmid.2019.102419
Received 22 December 2018; Received in revised form 18 June 2019
Available online 25 June 2019
0147-619X/

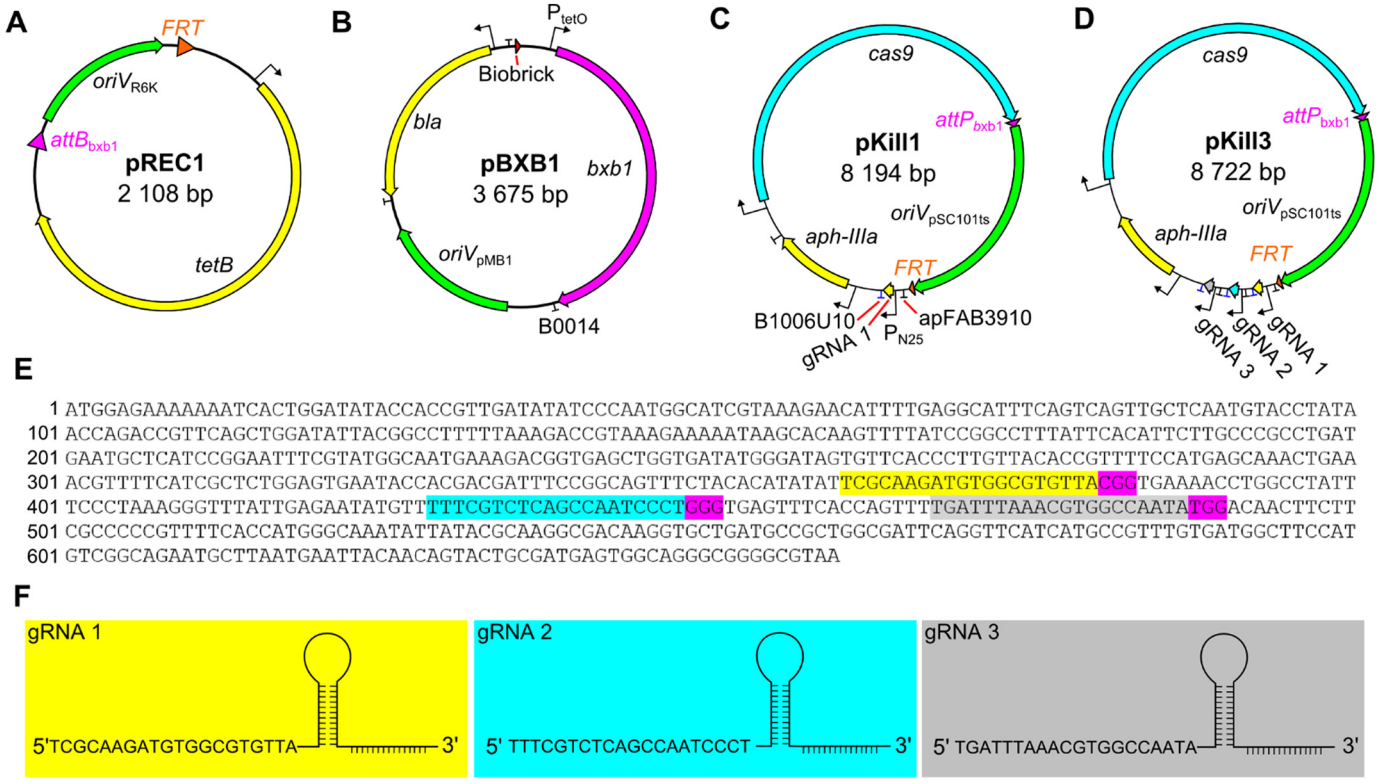

Fig. 1. Plasmid maps and design. Maps of pREC1 (A), pBXB1 (B), pKill1 (C) and pKill3 (D) are shown to scale. Total size of the plasmid in base pair (bp) is displayed below the plasmid name. Promoters and terminators of the gRNAs from pKill3 are identical to pKill1's gRNA. E, complete coding sequence of the target chloramphenicol resistance gene *cat* with the protospacers highlighted in yellow (gRNA 1), blue (gRNA 2) and gray (gRNA 3) and their corresponding PAM highlighted in purple. F, schematic representation of each gRNA with the sequence of their spacers. The gRNA number and colour are conserved between panels. (For interpretation of the references to colour in this figure legend, the reader is referred to the web version of this article.)

with increasing numbers of DNA fragments to assemble, usually limiting them to about 6 DNA fragments. The total size of the plasmid also can decrease cloning efficiency, generally limiting these techniques to constructs of < 20 kbp. Furthermore, these protocols often rely on the PCR amplification of several DNA fragments to assemble, each of which are limited by the length of DNA amplifiable by PCR. *In vivo* DNA recombination-based techniques such as Recombineering (Datsenko and Wanner, 2000; Datta et al., 2006), Gene doctoring (Lee et al., 2009), or NO-SCAR (Reisch and Prather, 2015) can delete large DNA fragments. However, the size of the DNA molecule that can be introduced is limited as insertion of DNA fragment larger than 2.5 kbp using these techniques greatly decreases their efficiency (Kuhlman and Cox, 2010). Alternative recombination based techniques for the fusion of large DNA fragments (> 4 kbp) such as ALFIRE (Rivero-Muller et al., 2007) exists, but are time-consuming (Zhao et al., 2011) and often rely on counter selections with toxic genes that can quickly mutate, leading to variable recombination efficiencies. Consequently, there is a need for more efficient tools facilitating the manipulation of large DNA molecules such as conjugative plasmids that are often too large (> 20 kbp) to conveniently modify using *in vitro* DNA assembly techniques, particularly for the insertion of large (> 4 kbp) genetic cargos that often depend on recombineering.

Here, we present the Double Recombinase Operated Insertion of DNA (DROID) method, a novel DNA assembly strategy that allows the size-independent fusion of DNA molecules with high efficiency. DROID takes advantage of two sets of recombination sites to join DNA molecules without accumulating antibiotic markers. We exemplify the DROID assembly method by loading CRISPR-Cas9 systems into TP114, a conjugative plasmid of incompatibility group I2 (IncI2) (Grindley et al., 1972). We also show that the delivery of a CRISPR-Cas9 system by TP114 can cure a specific multicopy resistance plasmid in a target bacterium thus confirming the functionality of genetic payload introduced by DROID.

2. Material and methods

2.1. Bacterial strains, plasmids and growth conditions

Bacterial strains and plasmids used are described in Table S1. Cells were typically grown in Luria broth Miller (LB) or on Luria broth agar Miller (LBA) medium supplemented, when needed, with antibiotics or medium additives at the following concentrations: ampicillin 100 µg/mL, chloramphenicol (Cm) 34 µg/mL, diaminopimelic acid (DAP) 57 µg/mL, kanamycin (Km) 50 µg/mL, nalidixic acid 4 µg/mL, spectinomycin 100 µg/mL, streptomycin 50 µg/mL, and tetracycline 15 µg/mL. Conjugation experiments were performed between two modified strains of *Escherichia coli* Nissle 1917 (EcN) on LBA plates without antibiotics at 37 °C for 2 h unless specified otherwise in the figure legend. Cells were then resuspended, diluted and plated by spotting 5 µL of each dilution in triplicate on selective LBA plates. All cultures were grown at 37 °C, except for bacteria bearing thermosensitive plasmids (pE-FLP, pKill1, pKill3) which were grown at 30 °C. Bacterial cultures used in the experiments were grown for no > 18 h.

2.2. DNA manipulations

All primers used are described in Table S2. Plasmid DNA sequences were deposited in Genbank, accession number can be found in Table S1. Plasmid DNA was purified using the EZ10 Spin Column Plasmid DNA Miniprep kit (BIOBASIC) while genomic DNA was purified using Quick-DNA Miniprep kit (ZYMO RESEARCH). DNA fragments for plasmid construction were amplified by PCR using the TransStart PFU Fly DNA

polymerase (CIVIC BIOSCIENCE). PCR products were purified using Ampure DNA XP (BECKMAN COULTER) following manufacturer's recommendations. DNA fragments were then pooled and assembled using NEBuilder Hifi DNA Assembly (NEB). Gibson assemblies were then treated with 0.5 µL *Dpn*I for 15 min at 37 °C to digest the DNA template. The mixture was then transformed into chemically competent *E. coli* EC100Dpir + as described previously (Green and Rogers, 2013).

For clone screening, isolated colonies were picked and inoculated in up to 100 µL of 5% p/v chelex beads. The mixture was then heated at 55 °C for 25 min and 100 °C for 10 min. The supernatant was used as a DNA template for PCR screening using the TaqB (ENZYMATICS) or OneTaq (NEB) DNA polymerases.

2.3. Construction of the loading docks pREC1 and pBXB1

The DNA fragments for pREC1 were amplified from pOSIP-TT for the *tetB* gene and pKD4 for the $oriV_{R6K}$. *FRT* and $attB_{Bxb1}$ sites were provided within the PCR priming oligonucleotides. Plasmid pBXB1 contains $oriV_{pMB1}$-*bla* (ampicillin resistance gene) from pSB1A3, and the *Bxb1* integrase gene from pRAD-module-G8-C1 (Bonnet et al., 2012). The P_{tetO} promoter controlling the expression of the Bxb1 integrase is constitutive since its repressor (*tetR*) is absent on the plasmid construct. The resulting plasmids maps of pREC1 are shown in Fig. 1.A and pBXB1 in Fig. 1.B.

2.4. Construction of the CRISPR-Cas9 modules pKill1 and pKill3

Two CRISPR-Cas9 modules, pKill1 (Fig. 1.C) and pKill3 (Fig. 1.D), were created. First, gRNAs were designed to target the Cm resistance gene *cat* (Fig. 1.E) using DNA 2.0 (ATUM) web-based software with *E. coli* K-12's genome as an off-target sequence. The most potent gRNA spacers (highest score based on the ΔG, off-target frequency) were then analyzed by BLASTn (Altschul et al., 1990) against the EcN donor strain and *Enterobacteriaceae* genomes to eliminate any candidate gRNAs with high off-targeting (< 2 mismatches). Three gRNAs (Fig. 1.F) identified by this bioinformatics strategy were cloned into two different CRISPR-Cas9 system bearing plasmids named pKill1 and pKill3. Plasmids pKill1 and pKill3 were obtained by Gibson assembly, with pKill1 carrying gRNA 1 and pKill3 carrying gRNA 1, 2 and 3. Both plasmids were assembled using a similar strategy combining the *cas9* gene from pCas9, the kanamycin resistance gene *aph-IIIa* from pKD4, and the $oriV_{pSC101ts}$ from pGRG36 (Table S2). The gRNA 1 was amplified entirely from a previous construct (pKN02), while the spacers of gRNA 2 and 3 were added in PCR primer tails. For pKill3, assembly tags were placed between each gRNAs to prevent miss-assembly due to the repetitive nature of this gene locus. Junctions between DNA segments were created by introducing short sequences in the PCR primers. The integrity of all gRNA sequences was confirmed by Sanger sequencing using the Plateforme de séquençage et de génotypage des génomes (Université Laval, QC, Canada). The activity of pKill plasmids was assessed by electroporation in EcN modified strain KN03 + pT (Target plasmid) and spread on LBA plates selecting pKill only or pKill + pT supplemented with 1% arabinose. Plasmid pT encodes the targeted Cm resistance gene *cat* and an arabinose inducible *gfp* gene. Plasmid curation can therefore be easily followed in the recipient and transconjugant by fluorescence and Cm resistance loss.

2.5. Loading CRISPR-cas9 into TP114 by DROID

The loading dock consisting of *FRT-tetB-*$attB_{bxb1}$ was amplified from pREC1 and inserted in TP114 by recombineering using pSIM7 as previously described (Datta et al., 2006). The modified TP114::*tetB* was first transferred by conjugation at 37 °C in *E. coli* MG1655Nx^R to purify it from potential contaminating wildtype TP114. Then, TP114::*tetB* was transferred at 30 °C into *E. coli* EC100D*pir* + bearing pBXB1 and one of the pKill plasmid. Cells were incubated overnight to allow the Bxb1-mediated insertion of the pKill plasmid into TP114::*tetB*. The resulting plasmids TP114::*tetB*-Kill1 and TP114::*tetB*-Kill3 were then transferred by conjugation at 30 °C to *E. coli* MG1655Nx^R. From this point on, the strains were grown at 37 °C to avoid any activity of the thermosensitive replication origin ($oriV_{pSC101ts}$) from the integrated payload that might destabilize TP114::*tetB*-Kill. *E. coli* MG1655Nx^R + TP114::*tetB*-Kill1 or TP114::*tetB*-Kill3 were then transformed by electroporation with pE-FLP (St-Pierre et al., 2013). The final TP114::Kill1 and TP114::Kill3 constructs were finally transferred by conjugation to EcN KN01Δ*dapA* for assessment of CRISPR-Cas9 activity.

2.6. Plasmid pT copy number determination

An overnight culture of KN03 + pT was diluted 1/50 in fresh LB broth and incubated at 37 °C. The culture was sampled at an OD_{600nm} value of 0.20, 0.80 and > 2.00 to obtain plasmid copy number in early, mid-exponential as well as stationary growth phases. The gDNA of each sample was extracted using the Quick DNA Miniprep Kit (ZYMO RESEARCH) and quantified using a NanoDrop spectrophotometer (THERMO FISHER SCIENTIFIC). All qPCR reactions were performed following the iQ SYBR Green Supermix guidelines (BIO-RAD). The primers used to amplify a portion of the *cat* gene from plasmid pT, and of the housekeeping gene *rpoB*, are listed in Table S2. After optimization, plasmid pT copy number was then determined for each test conditions (OD_{600nm} of 0.20, 0.80 and 2.00) as previously described (Anindyajati et al., 2016).

2.7. CRISPR-Cas9 module activity test

To test the activity of the CRISPR-Cas9 systems, TP114, TP114::Kill1 and TP114::Kill3 were transferred by conjugation in KN03 + pT. The cells were then plated on selective LB agar medium +1% arabinose to induce the expression of the *gfp* gene from the targeted plasmid pT. Colony GFP fluorescence was visualized with a Typhoon FLA 9500 (GE HEALTHCARE LIFE SCIENCE). GFP fluorescence was detected using a Low Pass Blue filter and a 473 nm laser while the brightfield image was taken with a Low Pass Red filter and a 635 nm laser. The fluorescent and brightfield images were merged using ImageFiji software (Schindelin et al., 2012). Then, the green fluorescent and non-fluorescent colonies were counted. Plasmid curing was assessed by plating transconjugants on normal or selective media for pT. The same procedure was performed for the highly similar but untargeted plasmid pNT, which bears an ampicilin resistance gene (*bla*) for selection instead of the *cat* gene.

2.8. Statistical analysis

Statistical significance was tested on the logarithmic value of the data by One-way ANOVA. Differences between two test groups were considered significant when the *P*-value was below 0.05. *P*-values are noted directly in the figures: ns ($P \geq 0.05$), * ($P < 0.05$), ** ($P < 0.01$) and *** ($P < 0.001$).

3. Results and discussion

3.1. DROID method rationale

DROID uses two recombinases to join two DNA molecules, independently of their respective sizes and without the need of cumulating antibiotic resistance markers. The two DNA molecules to combine during.

DROID are referred to as the “acceptor DNA molecule” and the “payload”. The acceptor DNA molecule is first equipped with a loading dock, composed of an $attB_{bxb1}$ site, a selection marker and an *FRT* site (Fig. 2.A). The acceptor DNA molecule is then able to recombine with virtually any payload containing a corresponding $attP_{bxb1}$ site. To

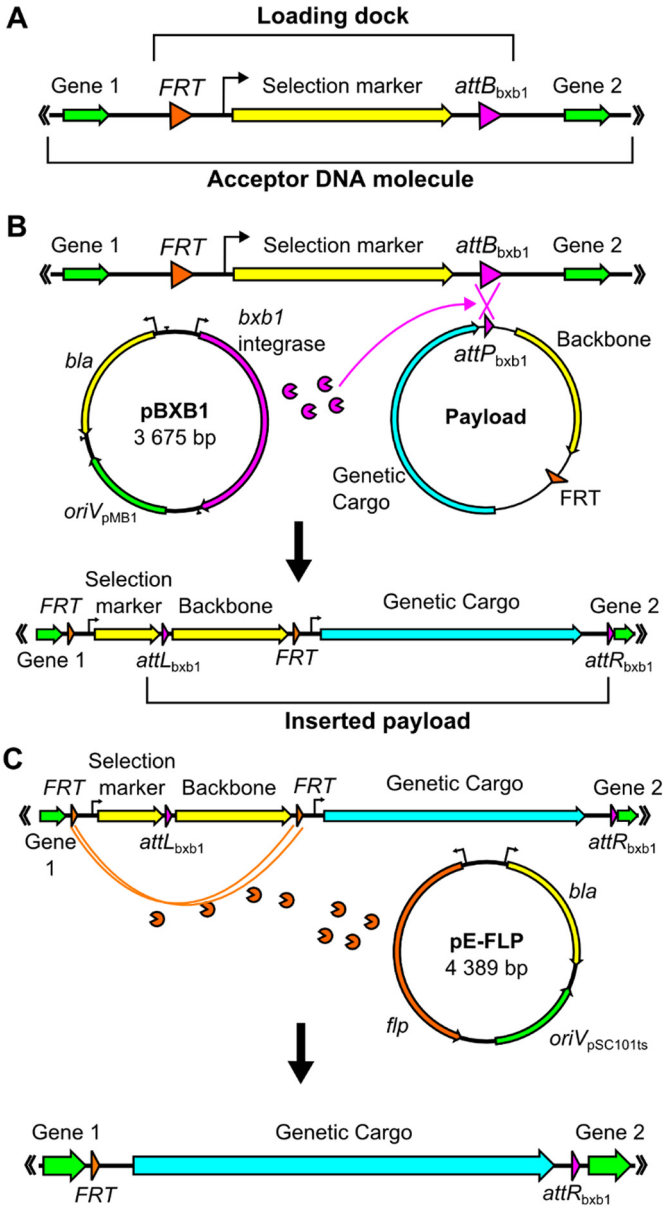

Fig. 2. Key steps of the DROID method. The DROID method mediates the fusion between an acceptor DNA molecule and a payload. A, the acceptor DNA molecule is a large construct that possess a loading dock, composed of an *FRT* site, a selection marker and an $attB_{bxb1}$ site. B, a helper plasmid expresses the Bxb1 integrase that recognizes the $attB_{bxb1}$ site on the loading dock and manages the recombination with the $attP_{bxb1}$ site from the payload. After recombination, the complete payload is inserted in the acceptor DNA molecule and is flanked by an *attL* and *attR* sites formed during the recombination process mediated by Bxb1. C, a helper plasmid then expresses the *flp* recombinase to promote the recombination between two FRT sites and remove all DNA sequences between them, in this case, the acceptor DNA molecule selection marker and the payload backbone. A-C, features are represented as arrows to facilitate the interpretation of insertion directionality.

promote recombination, the Bxb1 integrase (Bonnet et al., 2012) is expressed from a helper plasmid (pBXB1) and recognizes the $attB_{bxb1}$/$attP_{bxb1}$ pair (Fig. 2.B). After the integration of the genetic payload, two appropriately located *FRT* sites are recombined with the assistance of the Flp flipase expressed from pE-FLP. This second step removes any unnecessary genes from the final construction (Fig. 2.C) and deletes the $attL_{bxb1}$ site, preventing any excision of the genetic payload.

The DROID method is particularly useful when a genetic payload cannot be efficiently introduced using recombineering based techniques, and the acceptor DNA molecule is too large for easy *in vitro* manipulation. We chose to exemplify this situation by the insertion of a CRISPR-Cas9 system into the IncI2 TP114 conjugative plasmid. CRISPR-Cas9 systems (≥6.0 kbp) exceed the length recommended for effective recombineering while the size of TP114 (64,818 bp) is impractical for *in vitro* manipulation. Recombineering is a proficient method for the deletion of large fragments of DNA but its efficiency was shown to drop considerably for the insertion of DNA molecules larger than 2.5 kbp (Kuhlman and Cox, 2010). Considering that each recombineering step usually include a ~1 kbp antibiotic resistance gene, only ~1.5 kbp would remain available for the genetic payload to preserve good recombineering efficiency. This means that insertion of CRISPR-Cas9 in TP114 by recombineering would likely have to be divided in 5–6 steps, each requiring at least 2–3 days. In contrast, DROID allows the integration of a whole CRISPR-Cas9 system at once and is easily repeatable to allow fast gRNA switching and evaluation.

3.2. Insertion of the loading dock in TP114

Since TP114 doesn't include recombination sites essential for the DROID method, we first inserted a loading dock in this acceptor plasmid. The loading dock was designed to contain an *FRT* site, the *tetB* gene and the $attB_{bxb1}$ sequence. Plasmid pREC1 was created to contain this loading dock along with the $oriV_{R6K}$ replication origin, which maintenance depends on a chromosomally encoded replication initiation protein (Pi) (Fig. 1.A). This strategy was reported to lower the false positive recombinant rate in *pir-* hosts during the recombineering procedures(Datsenko and Wanner, 2000). The order and orientation of the recombination sites in the payload and acceptor DNA molecules must be designed carefully. Indeed, once inserted in the $attB_{bxb1}$ site, the payload will provide a *FRT* element that must be correctly aligned with the *FRT* located in the loading dock to allow the deletion of the *tetB* gene by Flp recombination.

The kanamycin resistance gene (*aph-IIIa*) of TP114 was chosen as the insertion point for the loading dock. The loading dock was amplified from pREC1 and inserted by recombineering into TP114, generating TP114::*tetB* (Fig. 3.A). The replacement of *aph-IIIa* by the loading dock *tetB* was confirmed by PCR (Fig. 3.B), and had no impact on TP114 conjugation efficiency (Fig. 3.C).

3.3. Engineering of two functional CRISPR-Cas9 systems

Two CRISPR-Cas9 systems were assembled to demonstrate the DROID method's ability to quickly introduce DNA payloads in TP114::*tetB*. Plasmid pKill1 (Fig. 1.C) contains the *cas9* gene along with one gRNA (gRNA #1) whereas plasmid pKill3 (Fig. 1.D) includes three gRNAs (gRNA #1, 2 and 3) instead. The use of pKill1 and pKill3 was interesting to determine if DNA payloads are prone to recombination during the DROID procedure since pKill3 contains three gRNAs composed of identical promoter and terminator sequences. All gRNAs were designed to target the Cm resistance gene *cat* (Fig. 1.E and F). Both pKill1 and pKill3 are otherwise identical, share the same selection marker, and were designed to facilitate the insertion of the CRISPR-Cas9 systems in TP114 by DROID. Importantly, pKill1 and pKill3 display impaired replication at ≥37 °C ($oriV_{pSC101ts}$), preventing possible instability at this non-permissive temperature after their insertion in TP114::*tetB*. Also, these CRISPR-Cas9 encoding plasmids carry the $attP_{bxb1}$ and the *FRT* sites that are located to allow the precise excision of the $oriV_{pSC101ts}$ after insertion in TP114.

Plasmid pT was next used to measure the activity of the CRISPR-Cas9 system by transformation of pKill1 and pKill3 into *E. coli* EC100D*pir* + bearing pT (Fig. 4.A). Plasmid pT includes the targeted *cat* gene in addition to an inducible *gfp* gene, and is present at high copy numbers (7–140 copies/cell), thus requiring robust expression of the CRISPR-Cas9 system for its curing. Transformation efficiency dropped drastically when selecting for the presence of both pT and the pKill

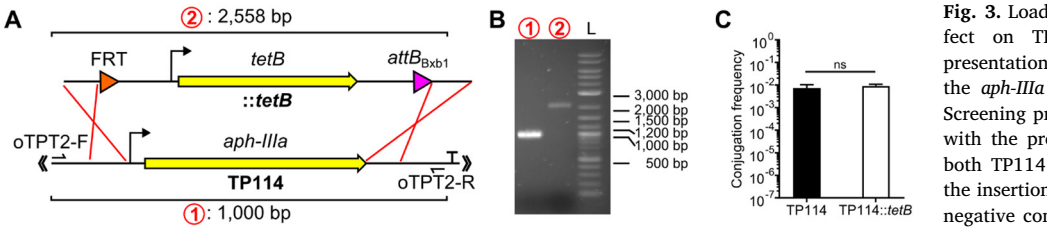

Fig. 3. Loading dock insertion have no negative effect on TP114 conjugation. A, schematic representation of the insertion of the loading dock in the *aph-IIIa* kanamycin resistance gene of TP114. Screening primers oTPT2-F and oTPT2-R are shown with the predicted size of amplified fragments for both TP114 and TP114::*tetB*. B, PCR screening for the insertion of the loading dock. Lane 1 is a TP114 negative control while lane 2 is a positive clone of TP114::*tetB,* lane L is a 1-Kb Plus DNA ladder (NEB). Lane numbers can be associated with the predicted size fragments depicted in panel A. C, conjugation rate after 2 h at 37 °C on LBA, as a function of the recipient bacteria CFU for both TP114 and TP114::*tetB* ($n = 3$). Statistical significance is indicated as follows: ns ($P > 0.05$), * ($P < 0.05$), ** ($P < 0.01$) or *** ($P < 0.001$). Bars represent the average value of the data while error bars show standard deviation.

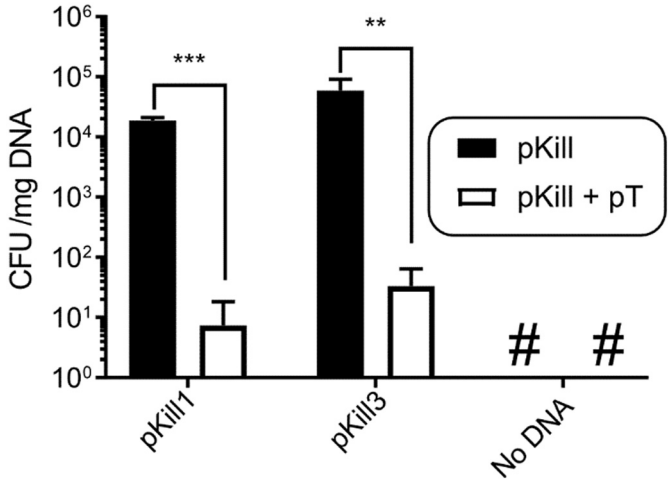

Fig. 4. The CRISPR-Cas9 systems plasmids pKill1 and pKill3 specifically cleave their target sequence. The number of pKill3 and pKill1 transformants was quantified in EcN KN03 bearing pT or not ($n = 3$). Selection of pKill transformants with and without co-selection for pT, a targeted chloramphenicol resistance plasmid. # denotes the absence of transformant colonies. Statistical significance is indicated as follows: ns ($P > 0.05$), * ($P < 0.05$), ** ($P < 0.01$) or *** ($P < 0.001$). Bars represent the average of the values with the error bar showing the standard deviation.

plasmid in the same cells. All pKill transformants without selection of pT showed no fluorescence, suggesting that these clones had all lost pT. Furthermore, subculturing of these non-fluorescent colonies ($n = 24$) in medium containing Cm showed no signs of growth, indicating Cm sensitivity. Taken together, these results indicate that the CRISPR-Cas9 system of pKill1 and pKill3 plasmids cleaves the targeted protospacers located on pT, leading to loss of the Cm resistance through plasmid curation.

3.4. Loading the CRISPR-cas9 systems on TP114::tetB

We next sought to insert the CRISPR-*cas9* systems pKill1 and pKill3 in the DROID-ready TP114::*tetB*. This step of the DROID method is mediated by the Bxb1 integrase, which is expressed from the pBXB1 helper plasmid. TP114::*tetB* and one of the pKill plasmids were introduced in *E. coli* EC100D*pir* + containing pBXB1 to catalyze their fusion (Fig. 5.A). To quantify the efficiency of the insertion step managed by Bxb1, the insertion of pKill in TP114::*tetB* was repeated in biological triplicates for both pKill1 and pKill3. The insertion of the pKill plasmids in TP114::*tetB* was confirmed by PCR screening (Fig. 5.B). A total of 46 clones of EC100D*pir* + bearing TP114::*tetB*, pBXB1 and a pKill plasmid were screened by PCR for insertion of the pKill plasmid in TP114 (Fig. 5.C). Although both TP114::*tetB* + pKill and TP114::*tetB*-Kill have the same antibiotic resistances, thereby preventing the selection for the insertion, most of the clones obtained showed a positive pattern for pKill insertion (27/46) and very few clones lacked a pKill insertion (4/46). These results demonstrate that Bxb1 can very efficiently recognize the $attB_{bxb1}/attP_{bxb1}$ pair and operate DNA fusion even in the absence of antibiotic selection pressure. Surprisingly, a high proportion of clones (15/46) contained a mixed population of TP114::*tetB* and TP114::*tetB*-Kill. The presence of these mixed population of TP114::*tetB* lacking or not the Kill insert in the same clonal colonies might indicate that, in those cells, TP114::*tetB* was present at a higher copy number than the pKill plasmid when the Bxb1 mediated fusion reaction took place. As the presence of uninserted pKill plasmid was not followed, it is also unclear if the Bxb1 integrase may have suffered from inactivating mutations throughout the insertion process, which could also explain this phenomenon. We also noted that the insertion of pKill1 appeared less efficient than the insertion of pKill3, suggesting that the efficiency of this step can vary between different genetic cargo plasmids. Nevertheless, 42/46 clones contained at least one copy of TP114::*tetB*-Kill and could therefore be used in further steps of the DROID method.

One clone per replicate of the pKill1 and pKill3 insertion in TP114::*tetB* was randomly selected and transferred by conjugation into *E. coli* MG1655Nx^R. Since the pKill plasmids encode a kanamycin resistance gene, their integration in TP114::*tetB* should lead to the mobilization of *aph-III*. Therefore, transconjugants were plated on LBA with or without kanamycin as a first assessment of pKill integration efficiency (Fig. 5.D). No significant difference was observed in the presence or absence of Km selection for pKill, thus revealing a high proportion of TP114::*tetB*-Kill in the transconjugant population in spite of the presence of a mixed population of TP114::*tetB* containing or not the Kill insert in the donor bacteria. We further investigated this result by subculturing transconjugant colonies recovered from LBA plates without Km onto solid medium supplemented with Km by replica plating and colony patching. Out of the 879 colonies replicated and 102 colonies patched, only 2 were unable to grow on Km plates selecting for pKill (Fig. 5.E). To confirm that Km resistance could be used to select for TP114::*tetB*-Kill, 41 Km resistant clones and the 2 Km sensitive clones were screened by PCR. All Km resistant clones showed the amplification product associated with the integrated form of pKill while the 2 Km sensitive clones were negatives (Fig. 5.F). The discrepancy between the results in Fig. 5C and figures 5DEF might be due to the cultivations steps preceding the transfer of TP114 to *E. coli* MG1655Nx^R. The overnight incubation at 37 °C of clones in LB selecting for both Tc and Km resistance might have favored the growth of daughter cells containing the TP114::*tetB*-Kill construct. Also, as PCR is not a quantitative technique, the presence of a mixed population of amplicon after PCR doesn't imply that these clones carried equal proportions of both constructs. Taken together, these results support the observation that the Bxb1 integration step in the DROID method mediates high-efficiency merging of two DNA molecules, without the need for selection nor extensive screening.

3.5. FLP mediated deletion of antibiotics markers

The last step of the DROID method is to use properly located *FRT* sites to eliminate any unwanted DNA from the final plasmid construct.

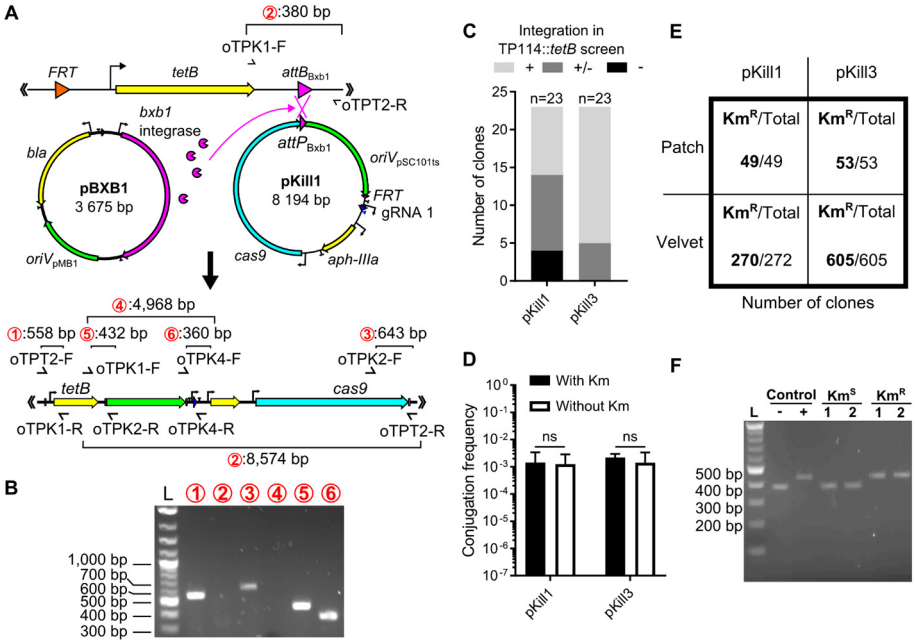

Fig. 5. Bxb1 allows efficient manipulation of large DNA molecules. A, schematic representation of pKill1 insertion. Screening primers are shown with the predicted length of their amplicon. B, PCR screening of pKill1 integrity after insertion in TP114. Amplicon numbering is consistent with panel A, lane L is a 1-Kb Plus DNA ladder (NEB). C, EC100D*pir* + pKill + pBXB1 + TP114::*tetB* colony PCR screening of pKill insertion in TP114::*tetB* using primers oTPK1-F, oTPK2-R and oTPT2-R. Clones presenting an amplicon corresponding to the integrated form of pKill were considered positive for pKill integration (+) while clones presenting the PCR pattern corresponding to TP114::*tetB* without the pKill insert were considered negative (−). Some clones displayed both the positive and negative PCR amplicon and were thus assigned to the +/− group. D, frequency of TP114::*tetB* (without Km selection) and TP114::*tetB*-Kill (with Km selection) transconjugants after a transfer from EC100D*pir* + to MG1655Nx^R (n = 3). Statistical significance is indicated as follows: ns ($P > 0.05$), * ($P < 0.05$), ** ($P < 0.01$) or *** ($P < 0.001$). Bar represent the means of the data with error bars being the standard deviation E, TP114::*tetB* transconjugant colonies from plates without Km were screened for presence of the pKill insert by replica plating (velvet) and colony patching (patch) on medium with and without Km. F, PCR screening of transconjugant colonies found to be Km^S or Km^R. Negative control was TP114::*tetB* purified DNA while the positive control was TP114::*tetB*-Kill1 purified DNA, lane L is a 1-Kb Plus DNA ladder (NEB).

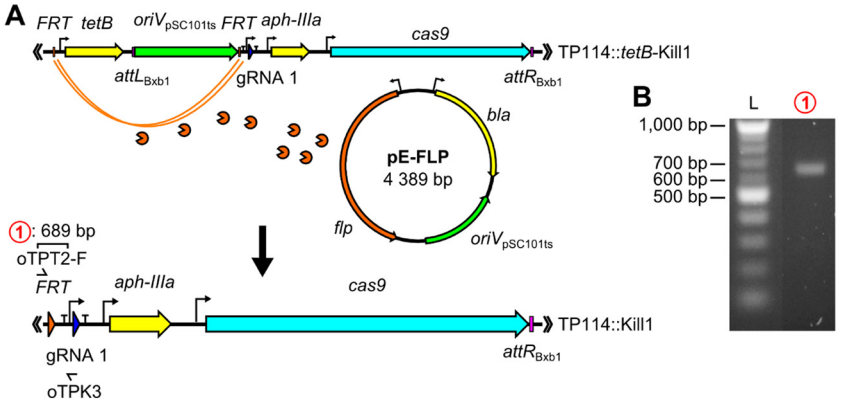

Fig. 6. The FRT recombination by the FLP flipase removes any unnecessary genes from the final construction. A, schematic representation of FLP mediated recombination of *FRT* sites. Primers used for PCR screening are shown with their predicted amplicon size B, PCR screening of FRT recombination using primers identified in panel A. Size of the amplified fragment is consistent with the amplicon of panel A, lane L is a 1-Kb Plus DNA ladder (NEB).

In the present case, the TP114::*tetB*-Kill construction contains two antibiotic selection markers and two origins of replication. As only one of each is required for full plasmid functionality, *FRT* sites were designed to eliminate the *tetB* resistance gene and *oriV*$_{pSC101ts}$. FRT recombination is performed by the Flp recombinase expressed from helper plasmid pE-FLP (Fig. 6.A). Transformation of pE-FLP led to loss of tetracycline resistance in all screened colonies (n = 12). The loss of both *tetB* and *oriV*$_{pSC101ts}$ was also verified by PCR (Fig. 6.B). The high efficiency of pE-FLP mediated *FRT* recombination in TP114::*tetB*-Kill is in good agreement with previous reports (St-Pierre et al., 2013). The integrity of gRNAs in TP114::Kill1 and TP114::Kill3 final constructs was next investigated by Sanger sequencing and revealed no mutation nor recombination, hereby showing that the DROID method doesn't promote recombination event within the DNA payload. Both TP114::Kill1 and TP114::Kill3 were next transferred in KN01Δ*dapA* for assessment of CRISPR-Cas9 functionality.

3.6. TP114 can perform in-cis mobilization of CRISPR-Cas9 systems

Both TP114::Kill1 and TP114::Kill3 can mobilize a CRISPR-Cas9 system to cleave the Cm resistance gene *cat*. To assess the functionality of the DNA payload after insertion in the acceptor DNA molecule by DROID, TP114, TP114::Kill1 and TP114::Kill3 were transferred by conjugation in a recipient strain (KN03) bearing plasmid pT. Curation was followed both by counting CFU on selective medium (Fig. 7.A) and loss of GFP fluorescence (Fig. 7.B). Transfer of TP114::Kill1 and TP114::Kill3 led to plasmid pT curation in most transconjugants. Moreover, transconjugants obtained using wild-type TP114 retained plasmid pT, indicating that the CRISPR-Cas9 systems were responsible for plasmid loss. Importantly, to verify the specificity of the CRISPR-Cas9 systems to the Cm resistance gene, the same experiment was repeated using plasmid pNT. This plasmid is highly similar to pT but encodes for ampicillin resistance instead of Cm resistance. TP114::Kill3, which is expected to show the highest off-targeting activity, was tested for its ability to cure pNT (Fig. 7.C). No difference was found in the number of transconjugants when selecting or not for pNT. This suggests that TP114::Kill3 had no off-targeting activity on pNT. Taken together, these results show that the CRISPR-Cas9 systems introduced in TP114 can be mobilized *in cis* while maintaining their activity and specificity.

3.7. DROID is a potent DNA assembly method that is readily adaptable to multiple applications

The DROID method efficiently joined two DNA molecules of 64 kbp and 8 kbp without the need for selection and extensive screenings. In our hands, the overall procedure took 14 days to complete (Table 1) and

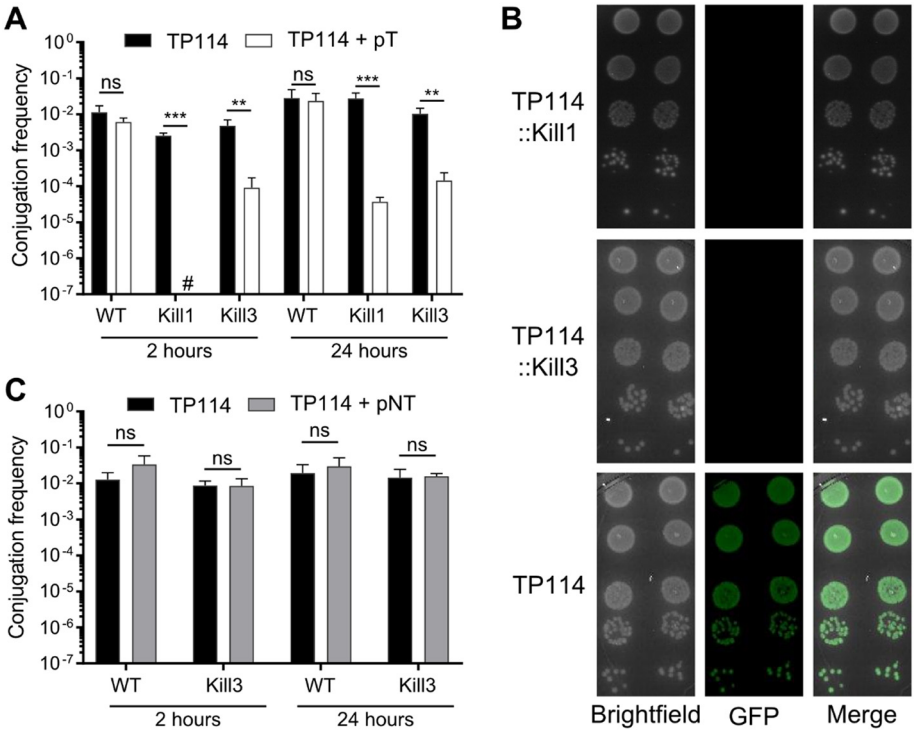

Fig. 7. TP114 can deliver functional CRISPR-Cas9 systems *in cis* to specifically cure an antibiotic resistance plasmid. A, conjugation of TP114 (WT), TP114::Kill1 (Kill1) and TP114::Kill3 (Kill3) from KN01ΔdapA to KN03 + pT. Transconjugants were selected for TP114 acquisition only (black) or co-selected for TP114 and pT (white). # denotes the absence of transformant colonies. B, representative colony picture of TP114::Kill1, TP114::Kill3 and TP114 transconjugants after 24 h of conjugation towards KN03 + pT without selection for pT. Plasmid pT is producing green fluorescence. C, conjugation of TP114 (WT) and TP114::Kill3 towards KN03 + pNT. Plasmid pNT is very similar to plasmid pT but does not include the targeted *cat* gene. Transconjugants were selected for TP114 acquisition only (black) or co-selected for TP114 and pNT (gray). A-C, Conjugation was performed over 2 and 24 h for all experiments with at least three independent biological replicates. Bars indicate the average value with error bars representing the standard deviation. Statistical significance is indicated as follows: ns ($P > 0.05$), * ($P < 0.05$), ** ($P < 0.01$) or *** ($P < 0.001$). (For interpretation of the references to colour in this figure legend, the reader is referred to the web version of this article.)

required minimal screening as each step produced a majority of clones carrying the expected product. Importantly, once the acceptor DNA molecule contains a loading dock, the procedure can be completed in as little as 7 days. Also, each step requires very little manipulation (~7 h of labor over 7 days). As such, the insertion of several different payloads in the acceptor DNA molecule could be performed in parallel.

While the DROID offers several advantages such as high efficiency, no DNA size limitation, and no undesired mutations resulting from the stimulation of recombination, the method also has certain limitations. First, DROID might not be advantageous to insert DNA payload < 5 kbp as most recombineering techniques could be completed faster with sufficient efficiency. Also, the current protocol of DROID implies that the acceptor DNA molecule must be mobilizable. While it is possible to mobilize very large DNA molecules (e. g. BACs), some applications such as the insertion of DNA in the chromosome of a bacterium cannot be performed with the current set of plasmids. To address this limitation, we generated a thermosensitive version of pBXB1 (pBXB1ts) to allow the loss of pBXB1ts by heat shock as opposed to conjugative transfer after the first step of the DROID. Furthermore, the procedure employs three antibiotic resistance genes to select for each of its components. In

Table 1
DROID protocol summary.

Main Steps	Insertion of the loading dock by recombineering	Bxb1 mediated insertion of the payload	FLP construction cleaning
Days	Day 1 to 5	Day 5 to 11	Day 11 to 14
Protocol	Transform the pSIM plasmid in an *E. coli* strain bearing the acceptor DNA molecule. Incubate cells overnight at 30 °C. (**Day 1**)	Transfer by conjugation the acceptor DNA molecule to the *E. coli* strain bearing pBXB1. Incubate the transconjugants selecting plate overnight at 30 °C. (**Day 5**)	Transform the *E. coli* strain bearing the assembly between the acceptor DNA molecule and the payload with pE-FLP. Incubate selective plates overnight at 30 °C. (**Day 11**)
	Parallelly, amplify the loading dock from pREC1 by PCR (x8), pool and purify the products by SPRI. (**Day 1**)	Pick a colony and subculture it in broth overnight at 30 °C. (**Day 6**)	Inoculate a colony in broth and verify by patching that it has lost the unwanted selective markers. Incubate the cultures overnight at 30 °C. (**Day 12**)
	Subculture a colony of transformants and incubate overnight at 30 °C. (**Day 2**)	Transform the payload in an *E. coli* strain with pBXB1 and the acceptor DNA molecule. Incubate the plate overnight at 30 °C. (**Day 7**)	Transfer the final construction to the strain of interest for payload mobilization. Incubate the transconjugants plate overnight at 37 °C.(**Day 13**)
	Perform recombineering as previously described (Datsenko and Wanner, 2000; Datta et al., 2006) (**Day 3**)	Pick a colony to inoculate in broth and incubate the culture overnight at 30 °C. (**Day 8**)	Subculture a single colony in broth for frozen stock. Screening for insert integrity is recommended at this step. (**Day 14**)
	Let cells recuperate overnight at 30 °C before plating on LBA selecting the loading dock insertion. (**Day 3**)	Transfer the acceptor DNA molecule to a plasmid free *E. coli* strain, selecting for transconjugants bearing the selection marker from the payload. Incubate transconjugant selecting plates overnight at 37 °C. (**Day 9**)	
	Confirm insertion by colony PCR and subculture positive clones for frozen stock. Proceed with the insertion of the payload. (**Day 4–5**)	Pick a colony for frozen stock generation. Proceed with the construction cleaning. (**Day 10–11**)	
Approximate hands-on time	10 h	4 h	3 h

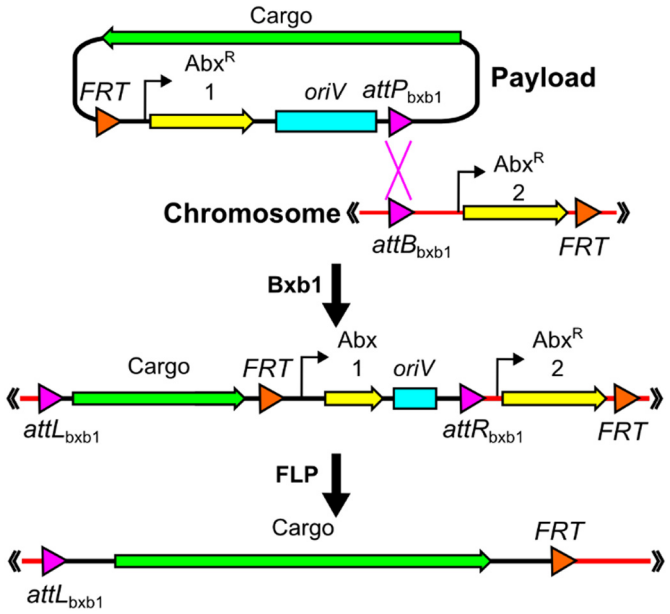

Fig. 8. Marker-free insertion of large payloads in the chromosome. A loading dock can be inserted in the chromosome of a bacteria. The chromosome of the bacteria is then considered as the acceptor DNA molecule and can be used to insert different payloads. The *FRT* and $attB_{bxb1}/attP_{bxb1}$ sites are placed so once the payload is inserted in the chromosome, both *FRT* sites can recombine and eliminate all antibiotics selection markers as well as the *oriV* from the payload. Number 1 and 2 are used to distinguish between two different genes sharing the same function. Abbreviations and designations: Abx^R, antibiotics resistance gene; *oriV*, origin of replication.

the present example, we used ampicillin resistance for pBXB1 and pE-FLP, tetracycline resistance for the loading dock and kanamycin resistance for the payload. We designed an alternative loading dock (pREC2) encoding chloramphenicol resistance instead of tetracycline to facilitate manipulation of systems bearing multiple resistance genes. Loading dock pREC1 was also designed to allow applications such as marker-free chromosomal insertions, which required minor changes to the recombination site placement (Fig. 8). One last limitation implies the use of homologous recombination for the insertion of the loading dock. Consequently, the insertion of the loading dock must be accomplished in a cell that can efficiently perform homologous recombination.

The DROID method could be further improved through many minor adjustments. First, as both recombination events present > 99% efficiency, performing both recombination steps at the same time could further accelerate the procedure. This modification could allow completion of DROID in < 5 days. Importantly, the usage of two or more orthologous $attB_{bxb1}/attP_{bxb1}$ sites could enable recursive insertions of payloads in a same acceptor DNA molecule. Such iterative DNA assembly could be used to assemble more complex DNA constructs like large metabolic pathways and even complete chromosomes.

4. Concluding remarks

The DROID method enables rapid, stable and size independent fusion of two DNA molecules. Here, we used DROID to rapidly insert CRISPR-Cas9 systems into a conjugative plasmid, and showed that the resulting molecule can serve as a delivery vehicle to efficiently suppress antibiotic resistance in targeted cells. As such, DROID facilitates to the development of microbiome engineering tools. Other types of genetic payloads such as genes encoding metabolic functions or anti-microbial peptides could be introduced in conjugative plasmids using DROID. This could help supplement the functions of the microbiota and potentially contribute to the treatment of dysbiosis. Finally, DROID could be readily adapted for other applications in synthetic biology that would require the assembly of two or more large DNA molecules.

Declaration of interest

The work presented in this manuscript is part of US provisional patent application 62/696,367.

Acknowledgments

This work was supported by the Canadian Institutes of Health Research (CIHR) (grant no. 159817) and by internal funds from the Université de Sherbrooke. S.R. holds a Chercheur boursier Junior 2 award from the *Fonds de recherche du Québec – Santé* (FRQS). K.N. acknowledges graduate research fellowships from the Fonds de recherche du Québec – Nature et technologies (FRQNT) and from the Natural Science and Engineering Research Council of Canada (NSERC). N.A. is supported by a doctoral scholarship from the Université de Sherbrooke. We thank Rodrigue lab members for thoughtful discussions and Alain Lavigueur for comments on this manuscript.

Appendix A. Supplementary data

Supplementary data to this article can be found online at https://doi.org/10.1016/j.plasmid.2019.102419.

References

Altschul, S.F., Gish, W., Miller, W., Myers, E.W., Lipman, D.J., 1990. Basic local alignment search tool. J. Mol. Biol. 215, 403–410. https://doi.org/10.1016/S0022-2836(05)80360-2.

Anindyajati, Anita, Artarini, A., Riani, C., Retnoningrum, D.S., 2016. Plasmid copy number determination by quantitative polymerase chain reaction. Sci. Pharm. 84, 89–101. https://doi.org/10.3797/scipharm.ISP.2015.02.

Bäckhed, F., Manchester, J.K., Semenkovich, C.F., Gordon, J.I., 2007. Mechanisms underlying the resistance to diet-induced obesity in germ-free mice. Proc. Natl. Acad. Sci. 104, 979–984. https://doi.org/10.1073/pnas.0605374104.

Bikard, D., Euler, C., Jiang, W., Nussenzweig, P.M., Gregory, W., Duportet, X., Fischetti, V.A., Marraffini, L.A., 2014. Development of sequence specific antimicrobials based on programmable CRISPR-Cas nucleases. Nat. Biotechnol. 32, 1146–1150. https://doi.org/10.1038/nbt.3043.Development.

Bonnet, J., Subsoontorn, P., Endy, D., 2012. Rewritable digital data storage in live cells via engineered control of recombination directionality. Proc. Natl. Acad. Sci. 109, 8884–8889. https://doi.org/10.1073/pnas.1202344109.

Cash, H.L., Whitham, C.V., Behrendt, C.L., Hooper, L.V., 2006. Symbiotic bacteria direct expression of an intestinal bactericial Lectin. Science (80-.e) 313, 1126–1130. https://doi.org/10.1126/science.1127119.Symbiotic.

Citorik, R.J., Mimee, M., Lu, T.K., 2014. Sequence-specific antimicrobials using efficiently delivered RNA-guided nucleases. Nat. Biotechnol. 32, 1141–1145. https://doi.org/10.1086/498510.Parasitic.

Cohen, S.N., Chang, A.C.Y., Boyert, H.W., Helling, R.B., 1973. Construction of biologically functional bacterial plasmids in vitro. Proc. Natl. Acad. Sci. 70, 3240–3244.

Datsenko, K.A., Wanner, B.L., 2000. One-step inactivation of chromosomal genes in *Escherichia coli* K-12 using PCR products. PNAS 97, 6640–6645.

Datta, S., Costantino, N., Court, D.L., 2006. A set of recombineering plasmids for gram-negative bacteria. Gene 379, 109–115. https://doi.org/10.1016/j.gene.2006.04.018.

Engler, C., Kandzia, R., Marillonnet, S., 2008. A one pot, one step, precision cloning method with high throughput capability. PLoS One 3, e3647. https://doi.org/10.1371/journal.pone.0003647.

Geu-flores, F., Nour-eldin, H.H., Nielsen, M.T., Halkier, B.A., 2007. USER fusion : a rapid and efficient method for simultaneous fusion and cloning of multiple PCR products. Nucleic Acids Res. 35, e55. https://doi.org/10.1093/nar/gkm106.

Gibson, D.G., Young, L., Chuang, R.-Y., Venter, J.C., Hutchison, C.A., Smith, H.O., 2009. Enzymatic assembly of DNA molecules up to several hundred kilobases. Nat. Methods 6, 343–345. https://doi.org/10.1038/nmeth.1318.

Green, R., Rogers, E.J., 2013. Chem. Transform. E. coli. Methods Enzymol. 529, 329–336. https://doi.org/10.1016/B978-0-12-418687-3.00028-8.Chemical.

Grindley, N.D.F., Grindley, J.N., Anderson, E.S., 1972. R factor compatibility groups. Mol. Gen. Genet. 119, 287–297.

Guthrie, L., Gupta, S., Daily, J., Kelly, L., 2017. Human microbiome signatures of differential colorectal cancer drug metabolism. Biofilms and Microbiomes 3. https://doi.org/10.1038/s41522-017-0034-1.

Kuhlman, T.E., Cox, E.C., 2010. Site-specific chromosomal integration of large synthetic constructs. Nucleic Acids Res. 38, e92. https://doi.org/10.1093/nar/gkp1193.

Lee, D.J., Bingle, L.E.H., Heurlier, K., Pallen, M.J., Penn, C.W., Busby, S.J.W., Hobman, J.L., 2009. Gene doctoring : a method for recombineering in laboratory and pathogenic Escherichia coli strains. BMC Microbiol. 9, 1–14. https://doi.org/10.1186/

1471-2180-9-252.
Ley, R.E., Backhed, F., Turnbaugh, P., Lozupone, C.A., Knight, R.D., Gordon, J.I., 2005. Obesity alters gut microbial ecology. Proc. Natl. Acad. Sci. 102, 11070–11075. https://doi.org/10.1073/pnas.0504978102.
Nobrega, F.L., Costa, A.R., Santos, J.F., Siliakus, M.F., Van Lent, J.W.M., Kengen, S.W.M., Azeredo, J., Kluskens, L.D., 2016. Genetically manipulated phages with improved pH resistance for oral administration in veterinary medicine. Sci. Rep. 6, 1–12. https://doi.org/10.1038/srep39235.
Nurmemmedov, E., Castelnovo, M., Medina, E., Catalano, C.E., Evilevitch, A., 2012. Challenging packaging limits and infectivity of phage λ. J. Mol. Biol. 415, 263–273. https://doi.org/10.1016/j.jmb.2011.11.015.
Penders, J., Stobberingh, E.E., Savelkoul, P.H.M., Wolffs, P.F.G., 2013. The human microbiome as a reservoir of antimicrobial resistance. Front. Microbiol. 4, 1–7. https://doi.org/10.3389/fmicb.2013.00087.
Reisch, C.R., Prather, K.L.J., 2015. The no-SCAR (Scarless Cas9 assisted Recombineering) system for genome editing in *Escherichia coli*. Sci. Rep. 5, 15096. https://doi.org/10.1038/srep15096.
Rivero-Muller, A., Lajic, S., Huhtaniemi, I., 2007. Assisted large fragment insertion by Red/ET-recombination (ALFIRE)— an alternative and enhanced method for large fragment recombineering. Nucleic Acids Res. 35. https://doi.org/10.1093/nar/gkm250.
Schindelin, J., Arganda-Carreras, I., Frise, E., Kaynig, V., Longair, M., Pietzsch, T., Preibisch, S., Rueden, C., Saalfeld, S., Schmid, B., Tinevez, J.Y., White, D.J., Hartenstein, V., Eliceiri, K., Tomancak, P., Cardona, A., 2012. Fiji: an open-source platform for biological-image analysis. Nat. Methods 9, 676–682. https://doi.org/10.1038/nmeth.2019.
Sender, R., Fuchs, S., Milo, R., 2016. Are we really vastly outnumbered ? Revisiting the ratio of bacterial to host cells in humans. Cell 164, 337–340. https://doi.org/10.1016/j.cell.2016.01.013.
St-Pierre, F., Cui, L., Priest, D.G., Endy, D., Dodd, I.B., Shearwin, K.E., 2013. One-step cloning and chromosomal integration of DNA. ACS Synth. Biol. 2, 537–541. https://doi.org/10.1021/sb400021j.
Van Schaik, W., 2015. The human gut resistome. Philos. Trans. R. Soc. B 370, 1–9.
Villarroel, J., Kleinheinz, K.A., Jurtz, V.I., Zschach, H., Lund, O., Nielsen, M., Larsen, M.V., 2016. HostPhinder : a phage host prediction tool. Viruses 6, 1–22. https://doi.org/10.3390/v8050116.
Yosef, I., Manor, M., Kiro, R., Qimron, U., 2015. Temperate and lytic bacteriophages programmed to sensitize and kill antibiotic-resistant bacteria. Proc. Natl. Acad. Sci. 112, 7267–7272. https://doi.org/10.1073/pnas.1500107112.
Zhao, Y., Wang, S., Zhu, J., 2011. Original article a multi-step strategy for BAC recombineering of large DNA fragments. Int J Biochem Mol Biol 2, 199–206.